Hyperaccumulation of phosphate by alfalfa (Medicago sativa) with targeted deletions in PHOSPHATE2 (PHO2) in high phosphate soil conditions

Kabita Poudel
Shaun J. Curtin
Deborah A. Samac
Craig C. Sheaffer
Daniel Schlatter
Joshua D. Gamble
Sheri Huerd
Zhanyou Xu

Zhanyou.Xu@usda.gov

USDA-ARS https://orcid.org/0000-0002-7633-036X

Research Article

Keywords: Phytoremediation, pho2 mutant, Gene editing, Phosphorus, Hyperaccumulator, Environmental Sustainability

Posted Date: June 11th, 2026

DOI: https://doi.org/10.21203/rs.3.rs-9891051/v1

Abstract

Background and Aims

Agricultural phosphorus (P) management is essential for maintaining crop yields, but practices aimed at preventing deficiency often result in overuse and soil P saturation. The subsequent runoff contributes to eutrophication of nearby water bodies. Phytoremediation, using plants to absorb excess soil nutrients, offers a sustainable solution but requires engineering crops that hyperaccumulate P. Recent genetic studies show that mutations in the *PHO2*-like genes, which help maintain phosphate (Pi) homeostasis, can result in substantial Pi hyperaccumulation in mutant plants.

Methods

In this study, mutated *pho2* alleles from the six-haplotype mutant PhotM65-2 were introgressed into elite genotypes of tetraploid alfalfa (*Medicago sativa* L.), resulting in seven F1 lines with mutations in *PHO2*-like genes (*PHO2-B* and *PHO2-C*). The study characterized these F1 mutants, evaluated their Pi accumulation, and identified the most effective genetic combinations for Pi accumulation.

Results

Specifically, double and triple mutants with edits in *PHO2-B* and *PHO2-C* accumulated significantly more Pi than control genotypes under both high and low P conditions. Notably, some novel mutants maintained enhanced Pi content in their leaves without a biomass penalty.

Conclusion

This study demonstrates the successful introgression of CRISPR/Cas-edited *PHO2-B/C* alleles in alfalfa, identifying specific mutated *pho2* allele combinations in F1 lines to create P-hyperaccumulator plants for remediating P-saturated soils and advancing agricultural sustainability.

Introduction

Phosphorus (P) is essential for plant growth, but its over-application has led to widespread soil saturation in farmlands. This excess P runs into waterways, driving eutrophication and creating dead zones that damage aquatic biodiversity and impose substantial economic costs (Downing et al. 2021; Scholz et al. 2025). Based on International Resource Panel (IRP) estimates, approximately 400 dead zones occur globally, covering an area roughly equal to that of the UK (UNEP 2021). If current climate and human population trends continue, eutrophication is projected to increase by 20–100% by 2050 and up to 120–390% by 2100 (Downing et al. 2021). In the United States alone, freshwater eutrophication costs approximately $2.2 billion annually (Dodds et al. 2009). Worldwide efforts to reduce P loss to freshwater from human sources are projected to cost roughly US $265 billion annually (Johnes et al. 2022) with associated social costs projected to reach $81 trillion by 2050 (Downing et al. 2021). These substantial economic and environmental burdens underscore the urgent need for effective P management strategies, including phytoremediation.

Phytoremediation, using plants to extract contaminants, is a cost-effective (Yadav et al. 2022) strategy for mitigating soil P pollution. While conventional methods can cost up to $252 per cubic meter of soil, phytoremediation averages just $0.02–$1.00 per cubic meter (Cunningham et al. 1995). Its advantages extend beyond cost: as a solar-powered process, it avoids secondary pollution and produces harvestable biomass. In the specific context of P remediation, harvested biomass can be repurposed as a biofertilizer. Unlike the phytoremediation of toxic trace elements or recalcitrant organics where biomass disposal requires strict containment, recycling P-enriched biomass facilitates more sustainable nutrient cycling. Nutrient recovery of remediated P supports a circular phosphorus economy and reduces reliance on finite mineral P reserves. These combined economic, environmental, and resource recovery benefits make it a superior sustainable remediation strategy. However, conventional crops typically absorb only 15–30% of applied P annually (Syers et al. 2008), making remediation impractically slow, potentially taking decades (Delorme et al. 2000). Improving the P acquisition efficiency of crops is therefore crucial for both productive agriculture and environmental protection (Campos et al. 2018).

Plants utilize root phosphate transporters (PHTs) to absorb inorganic phosphate (Pi) from the soil and transport it internally. To maintain Pi homeostasis, they rely on intricate signaling networks, particularly the essential PHO pathway (Zulfiqar et al. 2025). *PHO2*, which encodes the ubiquitin-conjugating enzyme (UBC24), serves as a regulatory checkpoint in the secretory pathway (Delhaize and Randall 1995). PHO2 proteins promote the degradation of PHT1 (PHOSPHATE TRANSPORTER 1) and potentially PHF1 (PHOSPHATE TRANSPORTER TRAFFIC FACILITATOR1) through ubiquitination, thereby decreasing the number of PHT1 proteins available at the plasma membrane for Pi uptake (Huang et al. 2013). The expression of *PHO2* gene is post-transcriptionally regulated by microRNAs, particularly miR399 (Bari et al. 2006). Its downstream targets include various phosphate transporters (PTs), RNases, acid phosphatases, and enzymes involved in lipid metabolism, all of which play a role in maintaining Pi balance within plants (Prathap et al. 2022). The transcription factor PHR1 positively regulates the expression of miR399. When internal Pi levels drop due to Pi starvation, PHR1 induces the upregulation of miR399, which then targets and cleaves the *PHO2* transcripts (Aung et al. 2006; Chiou et al. 2006; Bari et al. 2006). Decreased levels of PHO2 proteins lead to reduced ubiquitination of PHT1 proteins, allowing these transporters to reach the root plasma membrane without degradation and enhancing Pi uptake from the soil.

Mutations in the *PHO2* gene disrupt this Pi homeostasis, resulting in a hyperaccumulation of Pi in shoot tissues. This phenomenon was first identified in Arabidopsis through mutant screenings (Delhaize and Randall 1995; Dong et al. 1998; Aung et al. 2006) and later confirmed in rice (Hu et al. 2011), wheat (Ouyang et al. 2016), *Medicago truncatula* (Curtin et al. 2017), and strawberry (Zhang et al. 2023). Recently, this research has been successfully applied to tetraploid alfalfa, resulting in the development of the non-transgenic *pho2* mutant, PhotM65-2 (Miller et al. 2022), which exhibits enhanced Pi accumulation capabilities. The potential for multiple harvests makes alfalfa an effective candidate for Pi removal from soil, as it allows for the repeated harvesting of biomass with high Pi concentration. While the diploid model *Arabidopsis thaliana* possesses a single *PHO2* locus, the *Medicago* lineage underwent ancestral expansions resulting in three orthologs (*MtPHO2-A, -B, and -C*) in the diploid *M. truncatula*. In autotetraploid alfalfa (*M. sativa*, 2n = 4x = 32), (Miller et al. 2022) identified two primary orthologs situated on non-homologous chromosomes: *MsPHO2-B* on chromosome 2 and *MsPHO2-C* on chromosome 4. Given the autotetraploid nature of *M. sativa*, each locus is represented across four homologous chromosomes. These individual haplotypes are denoted as *MsPHO2-B1* through *B4* and *MsPHO2-C1* through *C4*. Although these haplotypes share fundamental regulatory roles, they are not genetically identical; alfalfa's high outcrossing rate and nucleotide diversity result in structural variations, including SNPs and small indels within coding and non-coding regions. In alfalfa, this high level of allelic redundancy across two unlinked loci creates significant functional buffering, necessitating the disruption of multiple haplotypes to reach the threshold required for altered Pi homeostasis and hyper-accumulation. PhotM65-2 carries mutations in all four haplotypes (*PHO2-B1, B2, B3* and *B4*) of the *PHO2-B* locus and in two haplotypes (*PHO2-C1* and *C3*) of the *PHO2-C* locus. This mutant line demonstrated higher Pi accumulation in its shoots than the wildtype control (Miller et al. 2022).

Despite these promising genetic advances, a significant translational gap remains. While donor lines like PhotM65-2 demonstrate high Pi accumulation (also written as concentration unless otherwise indicated) in leaves, their practical application is often limited by poor agronomic traits and field persistence. Furthermore, in the complex, autotetraploid genome of alfalfa, the optimal combinations of mutant *pho2* alleles for effective Pi accumulation in elite, commercially viable genetic backgrounds have not been systematically evaluated. This research aimed to introgress mutated alleles (*pho2-b* and *pho2-c)*, which are linked to enhanced Pi accumulation, into elite alfalfa genetic backgrounds through breeding and to assess F1 mutants for Pi accumulation. We hypothesized that targeted introgression of specific *pho2* mutant alleles into elite alfalfa germplasm would yield F1 mutants that maintain high Pi accumulation capacity without compromising agronomic fitness. Recent work in rice suggests that *PHO2* gene is a negative regulator of AMF symbiosis and that *pho2* mutants show earlier colonization by AMF and retain high AMF colonization in low P conditions (Birch et al. 2025). AMF populations are also likely to be depleted in soil with chronically high P levels where phytoremediation would be most valuable. Thus, we further postulated that inoculation with AMF may be especially useful in combination with alfalfa *pho2* mutants to expand their capacity to explore soil pore space to capture P.

To test these hypotheses, the present study had three primary objectives: (1) to generate and characterize a population of F1 alfalfa mutants by crossing the hyper-Pi accumulator donor PhotM65-2 with elite genotypes, creating diverse combinations of *pho2-b* and *pho2-c* mutant alleles; (2) to evaluate the Pi accumulation efficiency of these F1 mutants under different soil P conditions and in combination with AMF inoculation; and (3) to identify the most effective genetic combinations for Pi accumulation. By bridging the gap between a validated genetic mechanism and practical crop improvement, this work provides a strategy for developing improved alfalfa varieties capable of enhancing agricultural sustainability through the phytoremediation of P-enriched soils.

Materials and methods

Genetic crosses and population development

The F1 populations were generated by crossing PhotM65-2 with two elite alfalfa genotypes (S&W FD4 and Legacy FD4) with a fall dormancy (FD) 4, to evaluate effects of *pho2* mutations within a commercially relevant genetic background. Resulting seeds were harvested separately from each cross and subsequently used to establish the F1 populations (see Fig. 1). The genetics of F1 mutants and their mutant combination can be found in (Table 1). PhotM65-2 is a confirmed null-segregant (transgene-free) derived by segregating away the Cas9 T-DNA from the T1population and is carrying six specific mutations in the *PHO2* gene (four in the *PHO2-B* haplotype and two in *PHO2-C*), served as the male parent. PhotM65-2 carries one copy of *pho2-b1*, *pho2-b2, pho2-b3* and *pho2-b4*, two copies of *pho2-c1*, one copy of *pho2-c3*, and one wildtype *PHO2-C4* allele. The female parents (S&W FD4 and Legacy FD4) were established from single plants of elite breeding stock donated for research, which were subsequently clonally propagated. These elite parents represent current commercial alfalfa germplasm, with greater vigor and agronomic characteristics than RegenSY27x, the genotype used for initial plant transformation and gene editing.

Initial experiments in 2023 utilized a F1s from crosses with Legacy FD4 (M153-1) and S&W FD4 (M123-20) to confirm that the *pho2* mutation expresses a detectable phenotype in elite genetic backgrounds. The 2024 experiments focused on more mutant combinations derived from the crosses with S&W FD4. In these subsequent trials, S&W FD4 served as the primary wildtype control.

Genetic characterization of F1 mutants

Genotyping of the alfalfa *pho2* mutant plants was conducted using a series of haplotype-specific PCR and PCR-restriction fragment length polymorphism (PCR-RFLP) assays. RegenSY27x, the genotype used for original plant transformation, was utilized as the wild-type control for PCR and RFLP analysis. PhotM65-2 was used as the positive control for mutant detection.

The primers used to detect mutations in PhotM65-2, originally developed and described in (Miller et al. 2022), were used in this study (Supplementary Table S3). Briefly, to detect mutations in the *PHO2-B* and *PHO2-C* haplotypes, primers were designed to target unique junctions: the inversion mutation in *PHO2-B1* is identified by P1-F/P1-R, where P1-R only binds the inverted sequence; the 268-bp deletion in *PHO2-B2* is captured by P1-F/P5-R, where P5-R spans the deletion breakpoint; and the 3-bp in deletion *PHO2-B3* is specifically amplified by P1-F/P6-R, where P6-R spans the 3-bp deletion junction. Small mutations in *PHO2-B4* and *PHO2-C3* were confirmed via restriction digestion; the 7-bp mutation in *PHO2-B4* disrupts an *Eco*130I site, while the 1-bp insertion in *PHO2-C3* disrupts an *Xho*I site, rendering the mutant amplicons resistant to cleavage. Additionally, the 386-bp deletion in *PHO2-C1* is detected using P6-F/P8-R, where P6-F spans the deletion junction. Finally, the *PHO2-C2* and *PHO2-C4* haplotypes were confirmed through standard haplotype-specific amplification using the P11-F/P11-R and P10-F/P10-R primer sets, respectively. The genetics of F1 mutants and their mutant combinations can be found in (Table 1).

Soil preparation and AMF inoculation

To meet the experimental requirement for low baseline P, soil was collected 0–10 cm deep from two different agricultural fields in 2023 and 2024 located at the University of Minnesota Research and Outreach Center in Rosemount, Minnesota. Soil from these fields were pre-sampled and analyzed in both years for baseline nutrient content. Soil from fields having low P levels were selected for the study (Supplementary Table S1). Because the desired low-P baseline was detected in separate fields across the two years, the soil textures varied between the 2023 and 2024 trials. The soil was sieved (8 mm mesh) to remove debris and mixed with sand in a 1:1 (v:v) ratio to create a standardized growth medium. The soil-sand mixture was not sterilized to preserve the native soil microbiome. To simulate high-P conditions, P fertilizer was added to soil at 28 ppm P in 2023 and 60 ppm P in 2024. In 2023, both Triple Super Phosphate (TSP), a highly soluble P source, and Rock Phosphate (RP), a slow-release, less soluble source, were applied at 28 ppm P to compare the effects of fertilizer forms. Only TSP was used in the 2024 experiment at 60 ppm P. These rates were selected to exceed the University of Minnesota Extension recommendation for alfalfa (no fertilizer if soil P > 20 PPM Bray) and represent scenarios of P buildup. The soil was thoroughly mixed after fertilizer application to ensure homogeneity.

For the arbuscular mycorrhizal fungi (AMF) treatment, a commercial arbuscular mycorrhizal fungi (AMF) inoculant (Bio-Organics LLC), containing a consortium of nine species (*Glomus aggregatum*, *G. etunicatum*, *G. clarum*, *G. deserticola*, *G. intraradices*, *G.*

monosporus, *G. mosseae*, *Gigaspora margarita*, and *Paraglomus brasilianum*), was applied. In accordance with the manufacturer's instructions, a volume of 1 teaspoon (5 cc) was applied per pot as a band at two-thirds of the pot's depth during planting. This rate ensured a minimum of 50 propagules distributed across the nine species.

Transplantation and sample collection

F1 individuals as well as the S&W FD4 control were clonally propagated from 5 cm stem cuttings. The cuttings were placed in trays containing moist, medium-grade vermiculite. Trays were watered daily and maintained for 2 weeks to allow for root development. Following rooting, clones were carefully removed, their roots rinsed with water and transplanted into the prepared pots. Plants were maintained in a greenhouse under controlled conditions: 25°C day/18°C night temperature with a 14-hour photoperiod. All pots were watered daily with tap water as needed to maintain soil moisture.

Following the transplantation of clonally propagated plants, individuals were grown for one month and cut back once to promote uniform growth. They were then allowed to regrow for an additional month (totaling two months post-transplantation) prior to the first sampling event. For Pi quantification, single leaf from the same node position (excluding the petiole) were collected at the late vegetative stage. In the 2023 experiment, for each of the four sequential harvest cycles, the most recently expanded trifoliate leaves, specifically those from the second node from the shoot apex were collected from each plant. In the 2024 experiment, the sampling strategy was expanded to include nodal profiling; trifoliate leaves were collected from the second, fifth, and lowermost nodes of each stem. Leaf tissue samples for Pi analysis were immediately stored at -20°C. Following leaf sampling, the entire above-ground biomass was harvested, leaving the crown intact for regrowth. The harvest cycle was repeated every 30 days, with the exception of the second harvest cycle in 2024, where samples were collected on the 25th day to evaluate Pi accumulation at an earlier developmental stage. This approach allowed for the assessment of both temporal Pi accumulation and the spatial distribution of Pi within the plant architecture. At the final or fourth harvest, the aboveground biomass, crowns, and roots were harvested individually. Roots were washed with tap water to remove soil. All biomass samples were oven-dried at 60°C for four days, and dry weights were recorded. A subsample of fresh roots from each treatment was reserved for assessment of mycorrhizal colonization.

Experimental design

Independent greenhouse experiments were conducted over two years (2023 and 2024) to evaluate Pi accumulation in eight alfalfa genotypes: seven F1 *pho2* mutant lines and one elite genotype, S&W FD4, which served as the wildtype control. Both experiments followed a factorial design, with treatments randomized within the greenhouse.

The 2023 experiment used a 2 × 2 × 3 factorial designs to systematically test the effects of three variables: P fertilizer source, arbuscular mycorrhizal fungi (AMF) inoculation, and plant genotype on alfalfa performance. The fertilizer factor included two treatments: RP and TSP each applied at 28 ppm P. The AMF factor comprised two levels: either plants were inoculated with AMF (+ AMF abbreviated as A) or left uninoculated (–AMF abbreviated as N). For the genotype factor, three genotypes were used: the elite genotype S&W FD4 as control and two mutant lines, M123-20 and M153-1. This combination produced 12 unique treatment groups (2 P fertilizers × 2 AMF treatments × 3 genotypes). Each treatment group consisted of 30 replicate pots, each with a single plant, resulting in a total of 360 pots. To serve as baseline controls, an additional set of 18 pots (three genotypes × two AMF treatments × three replicates) was grown without fertilizer (NF).

In the 2024 experiment, the design was modified to a 2 × 2 × 7 factorial arrangement. The P fertilizer treatments were limited to either TSP applied at high P (60 ppm) or low P (0 ppm), while AMF conditions included inoculated and uninoculated plants. Seven genotypes were evaluated, consisting of the control S&W FD4 and six F1 mutant lines (Table 1). This led to 28 distinct treatment groups, each of which was replicated 15 times, for a total of 420 pots. As in the previous year, each pot was regarded as an independent experimental unit in all analyses with P treatment, genotypes, and AMF treatment considered fixed effects.

Soluble Pi measurement assay

The soluble inorganic phosphate (Pi) concentration in leaf tissues hereafter referred to as Pi accumulation was quantified using a colorimetric malachite green assay as previously described (Miller et al. 2022). Throughout this study, Pi accumulation was determined based on leaf Pi concentration, expressed as milligrams of Pi per gram fresh weight (mg Pi/ gFW or mg g^{-1}), unless

otherwise indicated. Pi concentration and Pi accumulation are used synonymously throughout the text unless otherwise indicated. For practical phytoremediation, where root harvesting is infeasible (Delorme et al. 2000) therefore our analysis focused on leaf Pi content as the key metric for Pi accumulation efficiency. Leaf samples were weighed individually and freeze-dried in 96-well storage tubes. A single steel bead was added to individual tubes and samples were homogenized using a tissue lyser set to 30 Hz for 30 seconds, repeated four times. Subsequently, 650 µL of deionized water was added to the homogenized powder, vortexed, and centrifuged (9,000 × g, 4 min). The supernatant was collected and stored at -20C.

Appropriate dilutions (1:5 or 1:10) of the supernatant were prepared to fall within the range of the standard curve. In a 96-well plate (Corning® 96 Well Black Polystyrene Microplate(Steen 1998; Johnston and Dawson 2005; Syers et al. 2008; Steffen et al. 2017), flat bottom clear), 5 µL or 2.5 µL of the diluted extract was combined with deionized water to a final volume of 25 µL. Then, 100 µL of 1 M HCl was added, followed immediately by 100 µL of color reagent [a 1:3 (v:v) mixture of 4.2% ammonium molybdate in 5 N HCl and 2% malachite green reagent]. After a 15-minute incubation at room temperature (20°C to 25°C), 100 µL of 1.5% Tween-20 was added, and the plate was incubated for an additional 15 minutes. Absorbance was measured at 660 nm using a microplate spectrophotometer. Sample Pi concentration (mg g^{-1}) was determined by comparison to a standard curve generated with a phosphate standard solution (Sigma-Aldrich, P3869).

AMF colonization assessment

Dried plant roots were subsampled and placed in biopsy cassettes. Cassettes were wetted, rinsed, and frozen until the time of staining (Grace and Stribley 1991). Ten to twenty cassettes were placed in a beaker with enough 10% KOH to generously cover them. Roots were autoclaved for 10 min, rinsed and acidified with HCL. Roots were stained for 6 min in hot 0.05% aniline blue stain and stored in 70% glycerol. Roots were examined under 200x magnification to quantify presence/absence of AMF structures (hyphae, vesicles, or arbuscles) (McGonigle et al., 1990).

Statistical analysis

All statistical analyses were conducted using R (Team 2009) software. Outliers were identified and removed before analysis using Interquartile Range (IQR) rule. Additionally, we removed data from individual plants that did not survive the duration of the experiment. The data were then analyzed using a three-way analysis of variance (ANOVA) to assess the main effects of P Fertilizer, AMF treatments, and genotype, as well as their interactions, on Pi accumulation and other measured traits. An ANOVA was conducted to determine the effect of the nodal position (second, fifth, and bottom node from the shoot meristem) on Pi accumulation. Following the ANOVA, Fisher's Least Significant Difference (LSD) post hoc tests were performed to determine significant differences among treatment means for each trait, with significance set at $\alpha = 0.05$.

Results

Introgression of mutant pho2 haplotypes into various alfalfa genotypes and their genotyping

The F1 populations were generated by crossing the gene edited genotype PhotM65-2 (male parent) with a high allelic dosage of *pho2* mutations (six out of eight haplotypes across the *PHO2 B* and *C* loci) with two elite alfalfa genotypes, S&W FD4 and Legacy FD4, to evaluate the *pho2* mutations within a high-vigor, commercially relevant genetic background (see details in Methods section and Fig. 1).

Figure 1 provides a schematic overview of the F1 mutation development workflow. Genomic DNA was extracted from leaf tissue of all F1 seedlings, the mutant parental line PhotM65-2 (T_1) and RegenSY27x. The inheritance of mutant *pho2* haplotypes was confirmed using a combination of haplotype-specific PCR and PCR-restriction fragment length polymorphism (PCR-RFLP) assays (Fig. 2), as previously developed for the donor parent (Miller et al. 2022). The specific primers and methods for each haplotype detection are detailed in (Material and Methods, Supplementary Table S2 and Supplementary Table S3). Briefly, the *pho2-b1 (pho2-b1:pho2-b1$^{\Delta 271inv}$)* mutation is defined by a 271-bp inversion in the *PHO2-B1* haplotype, while the *pho2-b2 (pho2-b2:pho2-b2$^{\Delta 268}$)* mutation is characterized by a 268-bp deletion in *PHO2-B2*. The *pho2-b3 (pho2-b3:pho2-b3$^{\Delta 3/1}$)* mutation is characterized by a 3-bp deletion and a 1-bp insertion in *PHO2-B3*. The *pho2-b4 (pho2-b4:pho2-b4$^{\Delta 7}$)* mutation features a 7-bp deletion in *PHO2-B4* that eliminates the *Eco* 130I restriction site. For the *PHO2-C* alleles, the *pho2-c (pho2-c1: pho2-c1$^{\Delta 386}$)* and *pho2-c3 (pho2-c3: pho2-c3$^{\Delta 1}$)*

mutants are defined by a 386-bp deletion and a 1-bp insertion in their haplotypes, respectively; in *PHO2-C3*, the 1-bp insertion causes loss of the *Xho* I restriction site. These distinct genetic markers allowed for precise identification of each mutant allele in the F1 plants. For mutant alleles *pho2-b1, pho2-b2*, *pho2-b3, and pho2-c1* the size of haplotype-specific PCR amplicon, similar to the donor PhotM65-2, directly indicated the genotype. For PCR-RFLP assays, the amplified product was digested with the appropriate restriction enzyme (*Eco* 130I for *PHO2-B4*; *Xho* I for *PHO2-C3*), and the fragments were resolved by gel electrophoresis. A mutant allele (*pho2-b4* and *pho2-b3*) was confirmed by the loss of the respective restriction site. Wild-type haplotypes for *PHO2-C2* and *PHO2-C4* were confirmed using allele-specific primers that only amplify the functional allele. This approach allowed precise determination of which F1 plants harbored specific *PHO2* mutations or wild-type alleles.

Table 1
Details of experimental controls, genotypes, crosses, mutations, and mutant notation.

Experiment year	Genotypes	Cross (Female* Male)	Mutant Genotype	Genotype Notation
2024	M123-1	S&W FD4 * PhotM65-2	*pho2-b1$^{\Delta 271inv}$/pho2-b2$^{\Delta 268}$/PHO2-B3/PHO2-B4/PHO2-C1/PHO2-C2/pho2-c3$^{\Delta 1}$/PHO2-C4*	*pho2-b1&2 /pho2-c3*
2024	M123-3	S&W FD4 * PhotM65-2	*PHO2-B1/pho2-b2$^{\Delta 268}$/pho2-b3$^{\Delta 3/1}$/PHO2-B4/pho2-c1$^{\Delta 386}$/PHO2-C2/ PHO2-C3/PHO2-C4*	*pho2-b2&3/pho2-c1*
2024	M123-7	S&W FD4 * PhotM65-2	*pho2-b1$^{\Delta 271inv}$/ PHO2-B2 / PHO2-B3/pho2-b4$^{\Delta 7}$/ PHO2-C /PHO2-C2/pho2-c3$^{\Delta 1}$/PHO2-C4*	*pho2-b1&3/pho2-c3*
2024	M123-18	S&W FD4 * PhotM65-2	*pho2-b1$^{\Delta 271inv}$/pho2-b2$^{\Delta 268}$/ PHO2-B3 / PHO2-B4/pho2-c1$^{\Delta 386}$/PHO2-C2/ PHO2-C3/PHO2-C4*	*pho2-b1&2 /pho2-c1*
2024	M123-19	S&W FD4 * PhotM65-2	*PHO2-B1/pho2-b2$^{\Delta 268}$/pho2-b3$^{\Delta 3/1}$/PHO2-B4/PHO2-C1/PHO2-C2/ PHO2-C3 /PHO2-C4*	*pho2-b2&3*
2024,2023	M123-20	S&W FD4 * PhotM65-2	*pho2-b1$^{\Delta 271inv}$/pho2-b2$^{\Delta 268}$ / PHO2-B3 / PHO2-B4/pho2-c1$^{\Delta 386}$/PHO2-C2/pho2-c3$^{\Delta 1}$/PHO2-C4)*	*pho2-b1&2 /pho2-c1&3*
2023	M153-1	Legacy FD4 * PhotM65-2	*PHO2-B1/pho2-b2$^{\Delta 268}$/pho2-b3$^{\Delta 3/1}$/PHO2-B4/pho2-c1$^{\Delta 386}$/PHO2-C2/pho2-c3$^{\Delta 1}$/PHO2-C4)*	*pho2-b2&3/pho2-c1&3*
2023,2024	S&W FD4	NA	NA	NA

Note: Δ denotes the mutation of the gene. Number in subscript above Δ denotes the number of base pairs mutated.

Effect of genotype in Pi accumulation

A three-way ANOVA revealed that genotype, fertilizer treatment, and their interaction had significant effects on Pi accumulation across all four harvests in both the 2023 and 2024 experiments (Supplementary Table S4 and Supplementary Table S5).

Post-hoc analysis of the 2023 experiment showed quadruple *pho2* mutant genotypes M123-20 and M153-1 exhibited higher leaf Pi accumulation relative to the wildtype control under TSP application (Table 2). The mutants, particularly M153-1, consistently outperformed the wild-type control in Pi uptake in most harvest time points when P was available. Under TSP conditions, the rank of Pi accumulation was generally M153-1 > M123-20 > S&W FD4. This confirms that the *pho2* mutation successfully enhances Pi concentration into the tissues compared to the control. For M153-1, leaf Pi accumulation was 37%, 25%, 17%, and 25% higher than the control across the four harvests. M123-20 showed increases of 27%, 14%, 11%, and 18% above the control at the respective harvests.

Table 2
Variation in leaf Pi accumulation (mg g^{-1}) among different genotypes at four-time points in the 2023 experiment.

2023	Harvest 1			Harvest 2			Harvest 3			Harvest 4		
Treatments	Fertilizer Treatment			Fertilizer Treatment			Fertilizer Treatment			Fertilizer Treatment		
Genotypes	NF	RP	TSP	NF	RP	TSP	NF	RP	TSP	NF	RP	TSP
S&W FD4	0.15 ± 0.03	0.23 ± 0.08	0.38 ± 0.14	0.20 ± 0.01	0.31 ± 0.08	0.42 ± 0.08	0.16 ± 0.04	0.29 ± 0.05	0.43 ± 0.10	0.20 ± 0.03	0.22 ± 0.04	0.33 ± 0.09
M123-20	0.15 ± 0.05	0.21 ± 0.05	0.53 ± 0.20	0.29 ± 0.04	0.30 ± 0.05	0.52 ± 0.11	0.26 ± 0.02	0.29 ± 0.07	0.50 ± 0.15	0.23 ± 0.04	0.25 ± 0.05	0.40 ± 0.12
M153-1	0.10 ± 0.02	0.23 ± 0.06	0.60 ± 0.21	0.24 ± 0.07	0.26 ± 0.06	0.65 ± 0.15	0.23 ± 0.02	0.25 ± 0.05	0.59 ± 0.16	0.17 ± 0.05	0.23 ± 0.07	0.47 ± 0.13
Fertilizer treatment	0.13 ± 0.04[C]	0.22 ± 0.06	0.51 ± 0.21	0.25 ± 0.05	0.29 ± 0.07	0.53 ± 0.15	0.21 ± 0.05	0.28 ± 0.06	0.50 ± 0.16	0.20 ± 0.04	0.23 ± 0.06	0.40 ± 0.12
Harvest time point	0.36 ± 0.21[B]			0.41 ± 0.16[A]			0.39 ± 0.16[A]			0.31 ± 0.12[C]		

Data represent mean leaf Pi concentration (mg g^{-1}) ± standard deviation under three phosphorus regimes: No fertilizer (NF), rock phosphate (RP) and triple superphosphate (TSP) averaged across AMF treatments. Within each harvest column, lowercase superscript letters denote significant differences among genotypes under the same treatment and uppercase superscript letters denote significant differences among NF, RP and TSP treatments within a specific genotype and harvest (LSD test, $P < 0.05$).

Analysis of the 2024 experiment confirmed F1 mutants showed variation in Pi accumulation across all four harvests ($P < 0.05$) (Table 3), reinforcing the trends observed in 2023. Most of F1 mutants consistently had higher Pi accumulation than the wild-type control in Pi uptake under high P fertilizer application. Triple mutants (M123-1, M123-3, M123-18) and the quadruple mutant M123-20 all consistently accumulated more leaf Pi than the control S&W FD4, but their peak values were lower than those of M123-7 and M123-19. Specifically, the double mutant M123-19 (*pho2-b2&b3*) and the triple mutant M123-7 (*pho2-b1&b3 / pho2-c3*) emerged as the top performers, showing similar or significantly higher Pi accumulation than the quadruple mutant (M123-20). At the first harvest, these two genotypes exhibited a striking 48–49% increase in Pi concentration compared to S&W FD4 (Table 3). This trait was maintained throughout the experiment, with M123-7 showing the highest relative accumulation compared to the control at the second (52% higher) and third (61% higher) harvests.

Table 3
Variation in leaf Pi accumulation (mg g^{-1}) among different genotypes at four time points in 2024.

Genotype	Harvest 1		Harvest 2		Harvest 3		Harvest 4	
	NF	TSP	NF	TSP	NF	TSP	NF	TSP
S&W FD4	0.42 ± 0.13	1.13 ± 0.36	0.16 ± 0.08	0.35 ± 0.21	0.40 ± 0.21	0.70 ± 0.34	0.47 ± 0.22	0.99 ± 0.47
M123-1	0.71 ± 0.35	1.40 ± 0.21	0.27 ± 0.13	0.52 ± 0.32	0.68 ± 0.43	1.08 ± 0.59	0.49 ± 0.22	0.99 ± 0.53
M123-3	0.47 ± 0.12	1.37 ± 0.31	0.20 ± 0.08	0.50 ± 0.26	0.51 ± 0.25	1.12 ± 0.43	0.60 ± 0.20	1.20 ± 0.49
M123-7	0.53 ± 0.27	1.88 ± 0.38^{A}	0.23 ± 0.09	0.64 ± 0.28	0.53 ± 0.28	1.55 ± 0.58	0.60 ± 0.29	1.43 ± 0.45
M123-18	0.48 ± 0.15	1.45 ± 0.46	0.20 ± 0.08	0.49 ± 0.24	0.87 ± 0.21	1.06 ± 0.45	0.50 ± 0.24	1.02 ± 0.49
M123-19	0.52 ± 0.30	1.89 ± 0.41	0.19 ± 0.12	0.69 ± 0.33	0.42 ± 0.31	1.30 ± 0.73	0.51 ± 0.28	1.51 ± 0.66
M123-20	0.43 ± 0.08	1.58 ± 0.31	0.16 ± 0.07	0.49 ± 0.18	0.38 ± 0.18	1.00 ± 0.30	0.50 ± 0.15	0.99 ± 0.43
Mean	0.96 ± 0.61^{A}		0.32 ± 0.24^{C}		0.72 ± 0.50^{B}		0.78 ± 0.50^{B}	

Data represent mean leaf Pi concentration (mg g^{-1}) ± standard deviation under two phosphorus regimes: no fertilizer (NF) and triple superphosphate (TSP) averaged across AMF treatments. Within each harvest column, lowercase superscript letters denote significant differences among genotypes under the same treatment and uppercase superscript letters denote significant differences between NF and TSP treatments within a specific genotype and harvest (LSD test, $P < 0.05$).

Effect of phosphorus fertilizer on leaf Pi accumulation

P fertilizer application had a pronounced impact on leaf Pi concentration in both years. The TSP treatments, both 28 ppm (2023 experiment) and 60 ppm (2024 experiment), consistently resulted in significantly higher Pi concentrations than RP or NF. In both 2023 and 2024 at all harvests, NF resulted in the lowest leaf Pi levels (Table 2, Table 3). For example, in 2023, S&W FD4 under TSP had highest Pi accumulation at the first harvest, while at RP and NF treatments were substantially lower. Mutant genotypes, such as M153-1 and M123-20, also showed their highest Pi values under TSP, often up to twice the values recorded for RP (Table 2). Furthermore, under TSP conditions, both mutants accumulated significantly more Pi than the wild-type S&W FD4, demonstrating that the *pho2* mutation effectively enhances Pi accumulation when provided with readily available P.

In 2024, the effect of the higher TSP treatment (60 ppm) was even more pronounced (Fig. 3). Across all genotypes and years, the TSP treatment nearly doubled Pi accumulation relative to NF (Table 2, Table 3). For example, highest Pi-accumulating mutant, M123-7, achieved a 3.55-fold increase in Pi accumulation compared to the NF treatment (Fig. 3).

Phosphorus fertilizer and genotype interaction influences Pi accumulation

A significant interaction was observed between genotype and P fertilizer rate and source (Supplementary Table S4, Supplementary Table S5). In 2023, Under NF and RP treatments, most genotypes showed similar accumulation, indicating limited genotypic differences when P availability was low (Table 2). In contrast, high P conditions (TSP treatment in both 2023 and 2024) led to greater differences among genotypes, with certain lines displaying much higher accumulation. While the S&W FD4 control line responded positively to TSP compared to RP in the 2023 experiment (as increase of 44–65% across four harvests in 2023), mutant lines benefited even more. M123-20 and M153-1 under TSP accumulated 19–39% and 40–58% more Pi, respectively, than the S&W FD4 control in sequential harvests (Table 2). When directly compared within genotype, M153-1 and M123-20 each accumulated more than 100% higher Pi under TSP than under RP treatments.

In 2024, the genotype effect was further amplified as all mutants showed substantial Pi gains under the high-P TSP regime; for instance, M123-7, M123-18, M123-19, and M123-20 noted relative increases of 200–300% in Pi compared to NF (Fig. 3). Most of the

mutant lines consistently accumulated higher Pi than the S&W FD4 control at every harvest under TSP (Table 3). At the initial harvest under TSP, the leaf Pi content of S&W FD4 increased by 175% relative to NF. Several mutant lines showed even greater relative increases. For instance, mutants M123-7, M123-18, M123-19, and M123-20 exhibited increases of 280%, 200%, 280%, and 300%, respectively in TSP relative to NF at first harvest (Fig. 3). Highly responsive genotypes, such as M123-7 and M123-19, demonstrated the greatest Pi accumulation under TSP, while NF treatments resulted in much lower Pi levels for all genotypes. The magnitude of genotype effect was amplified under high P availability, indicating a strong genotype × fertilizer interaction (Supplementary Table S5). Mutants grown with high P (60 ppm TSP in 2024) always accumulated more Pi than those grown with low P (28 ppm TSP or RP in 2023. Thus, both fertilizer source and genotype selection are critical factors for maximizing leaf Pi accumulation in alfalfa.

Higher Pi accumulation in selected mutants under no-fertilizer conditions

The triple mutant genotype M123-1(*pho2-b*$^{1\&2}$ */pho2-c*^{3}) consistently accumulated higher Pi than the control S&W FD4 at the first, second and third harvest under the NF treatment (Table 3). Other mutant lines including M123-7, M123-19, M123-18, and M123-3 also demonstrated higher Pi than the control under the NF treatment at various harvests, although the difference was not statistically significant at every time point. For mutants M123-7 and M123-19, Pi concentrations exceeded those of the control in first and fourth harvest, indicating their enhanced Pi accumulation efficiency under P-limited conditions (Table 3). These results highlight M123-1 (*pho2-b*$^{1\&2}$ */pho2-c*^{3}) as an optimal candidate for low-P environments, with additional mutant lines also offering improved Pi accumulation relative to the control at specific growth stages.

Phosphate accumulation displays a genotype-dependent response to fertilizer concentration

The impact of fertilizer type and concentration on Pi accumulation was assessed across the 2023 and 2024 experiments. The analysis focused on M123-20 and S&W FD4, as these genotypes were common to both study years. In 2023, under NF conditions at the first harvest, Pi concentrations were at their lowest and showed no significant difference between M123-20 and S&W FD4 (Table 2). However, at a 28 ppm TSP level, a significant increase in Pi accumulation was detected in both genotypes, where M123-20 significantly outperforming S&W FD4 (Table 2). A consistent trend was observed in 2024. Under NF conditions, leaf Pi accumulation remained low and statistically indistinguishable between M123-20 and S&W FD4 (Table 3). In contrast, the application of 60 ppm TSP resulted in a much more pronounced response in the mutant; M123-20 exhibited a 267% increase (3.67-fold change) in Pi accumulation compared to NF. This significantly surpassed the response of the wild-type S&W FD4, which showed only 169% increase (2.69-fold change) in Pi accumulation compared to NF.

The variation in soil physical properties between experimental years, specifically the transition from coarse-textured soil in 2023 to fine-textured soil in 2024 (Supplementary Table S1), resulted in a higher baseline Pi availability (Table 2 and Table 3). Fine-textured soils typically facilitate a higher nutrient flux to the root surface due to increased capillary action and surface area. Despite this shift in baseline, the relative performance of the genotypes remained constant. The *pho2* mutants (M123-20 and M153-1) consistently outperformed the wild-type S&W FD4 in Pi accumulation efficiency in 2023 (Table 2) and achieved significantly higher Pi concentrations in 2024 across a broader range of mutant lines (M123-1, M123-3, M123-7, M123-18, M123-19, and M123-20) (Table 3). This suggests that the physiological advantage conferred by the *pho2* mutation is robust across varying soil physical environments, which is a critical trait for the practical application of phytoremediation in diverse and unpredictable field conditions. These data demonstrate that while baseline accumulation is comparable between mutants and control genotypes under P-limitation (Table 2 and Table 3), the *pho2* mutation confers a significantly higher capacity for Pi accumulation when soil P availability is non-limiting. These data confirm that soil P availability is the main driver of leaf Pi content but also demonstrate a pronounced genotype-dependent response (Table 2 and Table 3). The mutant M123-20 displayed a significantly steeper increase in Pi than S&W FD4 as fertilizer concentration increased, indicating greater capacity of mutants for Pi translocation and accumulation under ample P supply.

Temporal dynamics of Pi accumulation

The factors of harvest time and genotype each individually exerted a significant influence on Pi accumulation ($P < 0.05$). However, the interaction between these two factors was not statistically significant (Supplementary Table S6). Analysis of Pi accumulation across four harvest time points revealed significant temporal variation (Table 2 and Table 3). The pattern of this variation differed

between the 2023 and 2024 experiments. In the 2023 experiment, mean Pi accumulation across all genotypes was highest at the second and third harvests. Levels were moderately high at the first harvest and showed a significant decline by the fourth harvest.

A distinct pattern was observed in the 2024 experiment. Here, Pi accumulation peaked at the first harvest, remained at comparable intermediate levels at the third and fourth harvests, but was significantly reduced at the second harvest. This anomalously low value at the second time point coincided with an early harvest date (25 days after the first harvest), which was before the development of flower buds (typically occurring at 32–34 days). This sampling was intentionally conducted at 25 days to capture the physiological status of the leaves at the terminal vegetative stage. This allowed us to distinguish the nutrient profile of a fully expanded vegetative canopy from the subsequent reproductive stage (Days 32–34), where nutrient partitioning dynamics shift significantly due to floral demand. Supporting this, nodal profiling indicated that at this early stage, Pi was predominantly localized at the fifth node, with limited translocation to new growth at second time point (Supplementary Figure S1).

Node-dependent Pi allocation

To assess spatial and temporal Pi allocation, we measured Pi concentration in leaves from three distinct nodes (second, fifth, and bottom node from the shoot meristem) across multiple harvests under NF and TSP treatments in the 2024 experiment. A clear interaction between fertilizer treatment, harvest time, and node position was observed. Under TSP fertilization, Pi levels were generally uniform across all nodes at most time points, indicating a sufficiency of P supply. In contrast, significant node-dependent variation in Pi accumulation occurred under NF conditions at the first time point harvest, revealing active redistribution (Fig. 4, Supplementary Figure S2). At the first harvest under NF, the leaf at the second (newest) node exhibited the highest Pi content across most genotypes, while the oldest node showed the lowest, suggesting preferential translocation of limited P to support new growth. This pattern shifted by the second harvest, where the mature leaf at the fifth node consistently accumulated the highest Pi levels in both NF and TSP treatments, coinciding with a sharp decrease in the leaf at the second node (Supplementary Figure S3). By the third harvest under NF, the leaves at the second and fifth nodes maintained similar, elevated Pi levels, reflecting a balance in nutrient distribution (Supplementary Figure S4). Under TSP, uniformity was generally maintained, though genotypic variations emerged (e.g., M123-3 and S&W FD4 showed elevated Pi in the leaf at the fifth node). At the final harvest, no significant differences in Pi concentration were detected among leaves for either fertilizer treatment (Supplementary Figure S5). These results demonstrate that Pi distribution is highly dynamic under limiting P conditions (NF), involving mobilization from older to younger tissues early in development, followed by accumulation in mature leaves. In contrast, adequate P supply (TSP) promoted uniform distribution throughout the plant, with some genotypic differences in allocation patterns.

Effects of genotype and AMF interaction on Pi accumulation

We evaluated the impact of arbuscular mycorrhizal inoculum application on Pi accumulation. Preliminary analysis of a subset of samples revealed low overall AMF colonization across all genotypes and P treatments, with no significant differences observed between *pho2* mutants and wild-type controls (data not shown). In the 2023 experiment, arbuscular AMF inoculation did not have a significant effect on Pi accumulation at the first two harvest time points. However, a significant main effect of AMF treatment emerged from the third harvest onward ($P < 0.05$). At this stage, plants inoculated with AMF exhibited a 7.3% higher mean Pi accumulation compared to non-inoculated controls. This effect was more pronounced at the fourth harvest, where AMF-treated plants showed an 11.8% increase in Pi accumulation.

In the 2023 experiment, a significant genotype and AMF as well as P and AMF interaction for Pi accumulation was detected at the third and fourth harvest time points ($P < 0.05$) (Supplementary Table S4). At these stages, under AMF inoculation, the mutant genotypes M123-20 and M153-1 accumulated significantly higher Pi than S&W FD4 (Table 4). In the absence of AMF, Pi accumulation was lower and statistically similar across all genotypes. By the fourth harvest, M153-1 also exhibited significantly higher Pi accumulation than S&W FD4 even in the non-inoculated treatment. At the third and fourth harvest time points, AMF inoculation did not improve Pi accumulation in plants fertilized with RP (Supplementary Figure S6 and Supplementary Figure S7). Interestingly, Pi accumulation was significantly ($P < 0.05$) higher in plants fertilized with TSP (Supplementary Figure S6, Supplementary Figure S7).

Table 4
Effect of arbuscular mycorrhizal fungi (AMF) inoculation on leaf Pi in (mg g^{-1}) in 2023.

Genotypes	First harvest		Second harvest		Third harvest		Fourth Harvest	
	AMF	No AMF	AMF	No AMF	AMF	No AMF	AMF	No AMF
S&W FD4	0.31 ± 0.15	0.30 ± 0.12	0.36 ± 0.10	0.36 ± 0.10	0.35 ± 0.12	0.36 ± 0.11	0.27 ± 0.10	0.27 ± 0.08
M123-20	0.37 ± 0.23	0.39 ± 0.24	0.43 ± 0.16	0.41 ± 0.14	0.42 ± 0.17	0.36 ± 0.12	0.37 ± 0.14	0.29 ± 0.08
M153-1	0.43 ± 0.26	0.40 ± 0.22	0.47 ± 0.24	0.44 ± 0.21	0.44 ± 0.23	0.39 ± 0.16	0.38 ± 0.22	0.32 ± 0.11
Mean	0.36 ± 0.22^{A}	0.36 ± 0.19^{A}	0.41 ± 0.17 ^{A}	0.40 ± 0.16 ^{A}	0.40 ± 0.19 ^{A}	0.37 ± 0.13^{B}	0.33 ± 0.15^{A}	0.28 ± 0.08^{B}

Data represent mean leaf Pi concentration (mg g^{-1}) ± standard deviation under two AMF regimes: No AMF and AMF pooled across fertilizer treatments. Within each harvest column, lowercase letters denote significant differences among genotypes under the same treatment and uppercase letters denote significant differences between AMF and no AMF treatments within a specific genotype and harvest (LSD test, $P < 0.05$).

Analysis of the 2024 data across seven genotypes revealed no significant main effect of AMF inoculation alone. However, a significant three-way interaction (Genotype × Phosphorus × AMF) was observed at the second, third, and fourth harvests ($P < 0.05$) (Supplementary Table S5).

TSP fertilization generally increased Pi accumulation. There was no specific pattern in Pi uptake among treatments and genotypes likely due to low AMF colonization. Specific interactions further illustrated this complexity in different harvest time points (Supplementary Figure S8, Supplementary Figure S9, Supplementary Figure S10, Supplementary Figure S11). For genotype M123-7 at the second harvest (Supplementary figure S9) and M123-1 at the fourth harvest (Supplementary figure S11), a significant difference in Pi accumulation between TSP and NF treatments was only observed when AMF was applied. For M123-19 at the fourth harvest (Supplementary figure S11), AMF inoculation under NF conditions increased Pi accumulation to a level that was not significantly different from the TSP treatment, whereas this difference was significant in the absence of AMF.

Biomass accumulation

In 2023, measurements across four harvests revealed that plants receiving TSP consistently had the highest biomass values, followed by RP, with the NF treatment having lowest biomass (Supplementary Table S7). S&W FD4 produced the highest aboveground biomass yield under TSP (Supplementary Table S7).

Across four harvest time points in 2024, TSP treated plants had greater biomass accumulation than the NF treatment at the second, third, and fourth harvest time points (Supplementary Table S8). Both the control (S&W FD4) and mutants, notably M123-18 and M123-20, achieved high biomass yields, particularly under TSP treatment (Supplementary Table S8). Importantly, at the third and fourth harvests, mutants M123-18 and M123-20 matched S&W FD4 in total biomass across both fertilizer treatments, suggesting that mutations conferring Pi hyperaccumulation do not compromise, and may even strengthen, agronomic performance under repeated harvest and varying nutrient regimes. This reveals their potential as breeding resources for high-performing, high-Pi accumulating alfalfa.

Also, we observed variability in resource allocation strategies among mutants. Some mutants like M123-1 and M123-20 showed higher root biomass under NF than TSP, indicating an adaptive response to seek nutrients under deficiency conditions (Supplementary Table S8). Alternatively, mutants like M123-7 and M123-18 maintained stable root biomass across NF and TSP, demonstrating resilience and resource allocation stability. Overall, AMF application did not promote growth in either the mutant or control alfalfa genotypes. A specific effect was observed only at the final harvest, where AMF application increased Pi accumulation in the control genotypes S&W FD4 and M123-7 under NF conditions.

Discussion

Conventional breeding techniques and genetic engineering can be used to boost the growth and biomass of hyperaccumulating species or to transfer these valuable traits into fast-growing plant varieties (DalCorso et al. 2019). This study demonstrates that stacking multiple mutations in *PHO2-B* and *PHO2-C* alleles in alfalfa leads to substantial increases in leaf Pi accumulation, especially under high fertilizer input (Table 3). Genotypes carrying combinations of *pho2-b* and *pho2-c* mutations, particularly M123-7 (*pho2-b1&3/pho2-c3*) and M123-19 (*pho2-b2&3*), consistently outperformed both the control and other mutant lines in Pi accumulation, underscoring the importance of gene dosage and the specific allelic combination for optimizing Pi accumulation and partitioning in aboveground tissues.

Previous research indicated that inorganic phosphorus (Pi) accumulation in alfalfa correlates positively with the number of mutations in the *PHO2-B* and *PHO2-C* genes; notably, single-haplotype disruptions fail to produce a discernible phenotype (Miller et al. 2022). However, the highest-accumulating original mutants exhibited severe growth stunting. To decouple this trait from biomass reduction, F1 hybrids were developed by crossing high-Pi male donors with high-vigor female parents. Because alfalfa is an autotetraploid with tetrasomic inheritance (Barcaccia et al. 2003), a maximum of four mutant alleles can be stacked in the F1 from a six-haplotype mutant donor (PhotM65-2) crossed with a wildtype plant. In 2023, experimental validation prioritized F1 lines that inherited the maximum possible mutant alleles to ensure trait penetrance. Lines M153-1 (*pho2-b2&b3 / pho2-c1&c3*) and M123-20 ((*pho2-b1&b2 / pho2-c1&c3*) were selected as "quadruple" mutants (carrying four mutant alleles), representing the upper limit of stable inheritance achieved from the initial parental crosses. As expected, the quadruple mutant (M123-20) demonstrated a higher capacity for Pi accumulation compared to the control. In 2024, the scope was expanded to include lines with varying allelic dosages to determine if a "sweet spot" exists achieving high Pi accumulation with fewer growth trade-offs. The tested cohort included: two mutant alleles: M123-19 (*pho2-b2&b3*), three mutant alleles: M123-1(*pho2-b1&b2 / pho2-c3*), M123-3 (*pho2-b2&b3 / pho2-c1*), M123-7 (*pho2-b1&b3 / pho2-c3*), M123-18 (*pho2-b1&b2 / pho2-c1)*, four mutant alleles: M123-20. This selection strategy facilitates the validation of the hyper-accumulation trait within a high-biomass genetic. More interestingly, under high P fertilizer conditions, both double (M123-19) and triple mutant (M123-7) outperformed not only the control but also the quadruple mutant (M123-20) in terms of Pi accumulation. This suggests that the specific combination of mutant alleles is more critical for optimal Pi accumulation than simply the number of mutations alone in the F1. A similar phenomenon was observed with the mutant characterization of *PHO2* in wheat where the correct balance of PHO2 proteins resulted in a favorable Pi trait (Ouyang et al. 2016).

Analysis of mutational impacts showed that mutants with at least two alleles mutated in *PHO2-B*, regardless of accessory *PHO2-C* mutations, outperformed the wild-type control in Pi accumulation. Detailed genotypic dissection revealed that mutant allele combination b1/b3 or b2/b3 (M123-7, M123-19) had a stronger response to Pi accumulation than b1/b2 (M123-1, M123-18, M123-20) based on overall ranking of genotypes for Pi accumulation (Table 3). This is consistent with previous studies indicating that Pi hyperaccumulation in mutants strongly correlates with *pho2-b* gene dosage, whereas the contribution of *pho2-c* alleles appears limited, likely reflecting the low and spatially restricted expression of *PHO2-C* in alfalfa. Also, studies in *Medicago truncatula* suggested that *MtPHO2-C* does not act as a functional ortholog of the *PHO2* gene previously described in other species, although evidence suggests it plays a secondary role in Pi homeostasis (Huertas et al. 2023). Additionally, M123-19 with two *pho2-b* mutations accumulated Pi at levels comparable to M123-7 with *pho2-b* and 1 *pho2-c* mutations and those of M123-20 with *pho2-b* and two *pho2-c* mutations, supporting the hypothesis that *PHO2-B* is key for regulating Pi homeostasis.

The higher baseline Pi observed across all genotypes in 2024 compared to 2023 may be attributed to differences in soil mineralogy and physical properties. Although both soils were categorized as low-P (Olsen P = 5 ppm), the 2023 soil was coarse-textured, whereas the 2024 soil was fine-textured (Supplementary Table S 1). Soil texture is known to significantly influence Pi mobility; fine-textured soils often provide better root-soil interface and higher moisture retention (Schoonover and Crim 2015), which facilitates the diffusion of Pi ions to the root surface. This likely explains the elevated Pi accumulation observed across all treatments in 2024, including the non-fertilized controls.

The 2023 data demonstrate that *pho2* mutants (M123-20 and M153-1) possess a significantly higher capacity for Pi accumulation than wild-type S&W FD4, particularly when provided with soluble P (TSP). Rock phosphate provided a moderate increase in tissue Pi compared to non-fertilized control (Table 2). The higher accumulation of Pi with TSP treatment compared to RP in both control and mutant lines underscores the critical role of P source solubility for maximizing plant nutrient uptake. TSP, being highly soluble, provides readily available Pi for root absorption, resulting in higher leaf Pi concentrations than RP, which is less soluble and therefore less accessible to the plant. This means that the extent to which a given genotype accumulates Pi is contingent upon environmental factors such as soil P availability (Table 2 and Table 3). Thus, deploying Pi-accumulating genotypes will be most effective when they

are well matched to the intended soil and management environment. For example, Pi accumulator mutant lines like M123-7 and M123-19 could be utilized in environments with high soil P for maximum nutrient accumulation. Mutants such as M123-1, which maintain elevated Pi levels even under no-fertilizer conditions, are candidates for sustainable agriculture or for use on marginal soils where P input is minimal or restricted. The observation that these mutants accumulate high Pi levels without toxicity symptoms suggests enhanced internal regulation, making them promising candidates for developing varieties that maximize both plant performance and Pi removal.

The S&W FD4 control consistently had greater biomass than the mutants in both shoots (Supplementary Table S7, Supplementary Table S8) and roots (Supplementary Table S9). In diploid plant species such as Arabidopsis and rice, loss of function of the *PHO2* gene was found to inhibit plant growth, possibly caused by the over-accumulation of Pi in shoots (Aung et al. 2006; Hu et al. 2011). We did not observe any Pi toxicity in F1 mutant plants. However, the reduced yield observed in F1 mutants may be attributed to hyperaccumulation as well as their substantial RegenSY27x background. Compounding this, the donor parent (PhotM65-2) developed via selfing of T_0 mutant PhotM65-2 exhibited significantly lower yield than RegenSY27x (Miller et al. 2022), likely due to inbreeding depression. Direct gene editing in elite alfalfa lines could serve as an alternative strategy to introduce the *pho2* mutation and the hyper-Pi accumulating phenotype directly into lines with high biomass potential. This approach would overcome the yield drag associated with low-performing genetic backgrounds, effectively streamlining the development of hyper-accumulating lines.

Despite these challenges, some F1 mutants such as M123-20 and M123-18 demonstrated higher Pi accumulation and comparable aboveground biomass yields to control genotypes at later harvests (Supplementary Table S7) highlighting the feasibility of selecting lines that combine high Pi accumulation with robust yield. Future improvement should focus on backcrossing or selective breeding of promising lines to balance Pi accumulation and biomass yield. For rigorous evaluation, future studies must assess biomass under field conditions simulating commercial production.

The effectiveness of arbuscular mycorrhizal fungi (AMF) inoculation on Pi accumulation was modest and strongly genotype dependent. This limited effect could be attributed primarily to low AMF root colonization rates (less than 20%) observed for both the control and mutant genotypes under low and high P conditions (data not presented). A notable increase in Pi accumulation due to AMF was detected only at later harvests for TSP application (20 ppm) (Supplementary Table S4 and Supplementary Table S5), suggesting that the establishment of the mycorrhizal symbiosis was both delayed and initially suboptimal. This positive response contrasts sharply with the results from RP application (28 ppm), where AMF inoculation provided little to no increase in Pi accumulation. The limited effectiveness of AMF with RP can likely be attributed to two interrelated factors: (1) the short duration of the experiment, which may have been insufficient for the slow process of RP solubilization and subsequent AMF-mediated transport to manifest, and (2) the inherent inefficiency of AMF in directly dissolving mineral phosphates. As supported by the literature (Salomon et al. 2022; Basiru and Hijri 2022; Berdeja et al. 2025), the variable performance of AMF inoculants in non-sterile soils may reflect the absence of specific phosphate-solubilizing bacteria (PSB), which are often crucial partners in a three-way symbiosis to liberate P from insoluble sources like RP. Further controlled research is required to examine the interactions between *pho2* mutants that are Pi hyperaccumulators, arbuscular mycorrhizal fungi, as well as other beneficial symbionts such as phosphorus-solubilizing bacteria.

High soil P levels are well-documented to suppress mycorrhizal colonization and function (Balzergue et al. 2013). Interestingly, in *Solanum lycopersicum* (tomato), loss of *PHO2* gene function inhibited the establishment of arbuscular mycorrhizal symbiosis (AMS) (Zeng et al. 2025). In contrast, studies in the rice and *Nicotiana benthamiana* reported that *pho2* mutants exhibited increased early AMF colonization (Birch et al. 2025). Given these conflicting results across species, further investigation is required to understand *PHO2* gene interactions with AMF in hyper-accumulating alfalfa. Understanding these interactions may offer valuable insights for enhancing Pi uptake and improving plant nutrient efficiency.

While the hyper-accumulation of Pi in *pho2* mutants represents a significant biotechnological milestone, greenhouse performance is an imperfect predictor of practical utility. Consequently, field validation is needed to determine the true agronomic and environmental value of these genotypes. Furthermore, the practical efficacy of these mutants in phytoremediation depends on the net 'P-removal rate' per hectare rather than tissue concentration alone, Consequently, future experiments must prioritize field-scale Pi accumulation studies to evaluate plant performance across diverse soil P gradients and multi-seasonal environmental fluctuations. Such validation is the final prerequisite for transitioning these mutants from greenhouse prototypes to functional tools for sustainable agriculture and phytoremediation.

Conclusion

This study demonstrated the feasibility of introgression of CRISPR/Cas edited *PHO2-B/C* genes in alfalfa, a critical step towards enhancing P use efficiency and phytoremediation capabilities in this important forage crop. Our detailed genotypic dissection identified specific mutant alleles with distinct, optimized functions: *pho2-b1&3/pho2-c3* and *pho2-b2&3* for Pi from enriched soil and triple mutants (*pho2-b1&b2 / pho2-c3)* for enhancing Pi accumulation in low-P soils. Notably, the *pho2-b1&3/pho2-c3* mutant proved most effective at maximizing Pi accumulation across varying soil P statuses. These results provide targeted breeding strategies for both agronomic improvement and environmental remediation. The concentration-dependent Pi accumulation in these engineered lines, combined with alfalfa's perennial growth and extensive root system, supports its development as a sustainable, dual-purpose platform for crop nutrition and soil phytoremediation. Collectively, these findings position hyperaccumulating alfalfa as a promising tool for sustainable P management and environmental stewardship.

Declarations

Author Contributions

K.P.: Project administration, Formal analysis, Validation, Visualization, Writing—original draft, Writing—review and editing.

S.J.C.: Supervision, Resources, Writing—original draft, Writing—review and editing

D.A.S.: Conceptualization, Resources, Writing—original draft, Writing—review and editing.
C.S.: Writing—original draft, Writing—review and editing.
D.S.: Methodology, Data analysis, Writing—review and editing.
J.D.G.: Methodology, Writing—review and editing.

S.H.: Data collection, Writing—review and editing.
Z.X.: Supervision, Resources, Analysis, Writing—original draft, Writing—review and editing.

All authors reviewed the manuscript.

Plant Material Statement

Our study complies with all relevant institutional, national, and international guidelines and legislation regarding plant research. The collection and experimental use of alfalfa (Medicago sativa L.) genotypes —including the elite breeding materials S&W FD4 and Legacy FD4, the genotype RegenSY27x, and the mutant donor parent PhotM65-2 were conducted in accordance with permissions obtained from the USDA-ARS Plant Science Research Unit in Saint Paul, MN. This research adheres to the IUCN Policy Statement on Research Involving Species at Risk of Extinction and the Convention on the Trade in Endangered Species of Wild Fauna and Flora (CITES).

The formal identification of the plant material used in this study was undertaken by Shaun J. Curtin at the USDA-ARS Plant Science Research Unit, in Saint Paul, MN. Plant materials were provided by the USDA-ARS Plant Science Research Unit as well as by S&W and Legacy seed companies and are publicly available upon request. A voucher specimen of alfalfa (*Medicago sativa* L.) hybrid Regen-SY germplasm has been deposited in the U.S. National Plant Germplasm System with the deposition number Reg. no. GP-242, PI 537440. The varieties S&W FD4 and Legacy FD4 are available through S&W and Legacy seed companies, respectively. The data that support the findings of this study are available from the corresponding author upon reasonable request.

Competing Interests
The author(s) declare no competing interests.

Funding

This work was supported by USDA-ARS Projects 5062-21000-035-000D and 5062-21500-001-000D.

Data Availability

The datasets generated during and/or analyzed during the current study are available from the corresponding author on reasonable request

Acknowledgements

This paper is a joint contribution from the Plant Science Research Unit, USDA-ARS, and the Minnesota Agricultural Experiment Station. Technical assistance from Mindy Dornbusch is gratefully acknowledged. Mention of any trade names or commercial products in this article is solely for the purpose of providing specific information and does not imply recommendation or endorsement by the U.S. Department of Agriculture. USDA is an equal opportunity provider and employer, and all agency services are available without discrimination.

References

1. Aung K, Lin SI, Wu CC, et al (2006) pho2, a phosphate overaccumulator, is caused by a nonsense mutation in a microRNA399 target gene. Plant Physiol 141:1000–1011. https://doi.org/10.1104/pp.106.078063
2. Balzergue C, Chabaud M, Barker DG, et al (2013) High phosphate reduces host ability to develop arbuscular mycorrhizal symbiosis without affecting root calcium spiking responses to the fungus. Front Plant Sci 4:. https://doi.org/10.3389/fpls.2013.00426
3. Barcaccia G, Tavoletti S, Mariani A, Veronesi F (2003) Occurrence, inheritance and use of reproductive mutants in alfalfa improvement. Euphytica 133:37–56. https://doi.org/10.1023/A:1025646523940
4. Bari R, Datt Pant B, Stitt M, Scheible W-R (2006) PHO2, MicroRNA399, and PHR1 Define a Phosphate-Signaling Pathway in Plants. Plant Physiol 141:988–999. https://doi.org/10.1104/pp.106.079707
5. Basiru S, Hijri M (2022) Does Commercial Inoculation Promote Arbuscular Mycorrhizal Fungi Invasion? Microorganisms 10:404. https://doi.org/10.3390/microorganisms10020404
6. Berdeja MP, Reynolds NK, Pawlowska T, Heuvel JEV (2025) Commercial bioinoculants improve colonization but do not alter the arbuscular mycorrhizal fungal community of greenhouse-grown grapevine roots. Environ Microbiome 20:15. https://doi.org/10.1186/s40793-025-00676-8
7. Birch S, Perryman S, Ellison EE, et al (2025) PHOSPHATE OVERACCUMULATOR 2 (PHO2) is a negative regulator of arbuscular mycorrhizal symbiosis
8. Campos P, Borie F, Cornejo P, et al (2018) Phosphorus acquisition efficiency related to root traits: Is mycorrhizal symbiosis a key factor to wheat and barley cropping? Front Plant Sci 9:1–21. https://doi.org/10.3389/fpls.2018.00752
9. Chiou T-J, Aung K, Lin S-I, et al (2006) Regulation of Phosphate Homeostasis by MicroRNA in *Arabidopsis*. Plant Cell 18:412–421. https://doi.org/10.1105/tpc.105.038943
10. Cunningham SD, Berti WR, Huang JW (1995) Phytoremediation of contaminated soils. Trends Biotechnol 13:393–397. https://doi.org/10.1016/S0167-7799(00)88987-8
11. Curtin SJ, Tiffin P, Guhlin J, et al (2017) Validating Genome-Wide Association Candidates Controlling Quantitative Variation in Nodulation. Plant Physiol 173:921–931. https://doi.org/10.1104/pp.16.01923
12. DalCorso G, Fasani E, Manara A, et al (2019) Heavy Metal Pollutions: State of the Art and Innovation in Phytoremediation. Int J Mol Sci 20:3412. https://doi.org/10.3390/ijms20143412
13. Delhaize E, Randall PJ (1995) Characterization of a Phosphate-Accumulator Mutant of Arabidopsis thaliana. Plant Physiol 107:207–213. https://doi.org/10.1104/pp.107.1.207
14. Delorme TA, Angle JS, Coale FJ, Chaney RL (2000) Phytoremediation of Phosphorus-Enriched Soils. Int J Phytoremediation 2:173–181. https://doi.org/10.1080/15226510008500038
15. Dodds WK, Bouska WW, Eitzmann JL, et al (2009) Policy Analysis Policy Analysis Eutrophication of U . S . Freshwaters : Damages. Environ Sci Technol 43:12–19
16. Dong B, Rengel Z, Delhaize E (1998) Uptake and translocation of phosphate by pho2 mutant and wild-type seedlings of Arabidopsis thaliana. Planta 205:251–256. https://doi.org/10.1007/s004250050318
17. Downing JA, Polasky S, Olmstead SM, Newbold SC (2021) Protecting local water quality has global benefits. Nat Commun 12:. https://doi.org/10.1038/s41467-021-22836-3

18. Grace C, Stribley DP (1991) A safer procedure for routine staining of vesicular-arbuscular mycorrhizal fungi. Mycol Res 95:1160–1162. https://doi.org/10.1016/S0953-7562(09)80005-1
19. Hu B, Zhu C, Li F, et al (2011) *LEAF TIP NECROSIS1* Plays a Pivotal Role in the Regulation of Multiple Phosphate Starvation Responses in Rice. Plant Physiol 156:1101–1115. https://doi.org/10.1104/pp.110.170209
20. Huang T-K, Han C-L, Lin S-I, et al (2013) Identification of Downstream Components of Ubiquitin-Conjugating Enzyme PHOSPHATE2 by Quantitative Membrane Proteomics in *Arabidopsis* Roots. Plant Cell 25:4044–4060. https://doi.org/10.1105/tpc.113.115998
21. Huertas R, Torres-Jerez I, Curtin SJ, et al (2023) Medicago truncatula PHO2 genes have distinct roles in phosphorus homeostasis and symbiotic nitrogen fixation. Front Plant Sci 14:1211107. https://doi.org/10.3389/fpls.2023.1211107
22. Johnes PJ, A L Heathwaite, Spears BM, et al (2022) Chapter 5. Phosphorus and water quality. https://doi.org/10.13140/RG.2.2.14950.50246
23. Johnston A, Dawson C (2005) Phosphorus in agriculture and in relation to water quality. Agricultural Industries Confederation Peterborough
24. McGONIGLE TP, Miller MH, Evans DG, et al (1990) A new method which gives an objective measure of colonization of roots by vesicular—arbuscular mycorrhizal fungi. New Phytol 115:495–501. https://doi.org/10.1111/j.1469-8137.1990.tb00476.x
25. Miller SS, Dornbusch MR, Farmer AD, et al (2022) Alfalfa (*Medicago sativa* L.) *pho2* mutant plants hyperaccumulate phosphate. G3 GenesGenomesGenetics jkac096. https://doi.org/10.1093/g3journal/jkac096
26. Ouyang X, Hong X, Zhao X, et al (2016) Knock out of the PHOSPHATE 2 Gene TaPHO2-A1 Improves Phosphorus Uptake and Grain Yield under Low Phosphorus Conditions in Common Wheat. Sci Rep 6:1–11. https://doi.org/10.1038/srep29850
27. Prathap V, Kumar A, Maheshwari C, Tyagi A (2022) Phosphorus homeostasis: acquisition, sensing, and long-distance signaling in plants. Mol Biol Rep 49:8071–8086. https://doi.org/10.1007/s11033-022-07354-9
28. Salomon MJ, Demarmels R, Watts-Williams SJ, et al (2022) Global evaluation of commercial arbuscular mycorrhizal inoculants under greenhouse and field conditions. Appl Soil Ecol 169:104225. https://doi.org/10.1016/j.apsoil.2021.104225
29. Scholz MJ, Obenour DR, Morrison ES, Elser JJ (2025) A critical eutrophication–climate change link. Nat Sustain 8:222–223. https://doi.org/10.1038/s41893-024-01507-3
30. Schoonover JE, Crim JF (2015) An Introduction to Soil Concepts and the Role of Soils in Watershed Management. J Contemp Water Res Educ 154:21–47. https://doi.org/10.1111/j.1936-704X.2015.03186.x
31. Steen I (1998) Phosphorus availability in the 21st century: management of a non-renewable resource. Phosphorus Potassium 217:25–31
32. Steffen MM, Davis TW, McKay RML, et al (2017) Ecophysiological Examination of the Lake Erie *Microcystis* Bloom in 2014: Linkages between Biology and the Water Supply Shutdown of Toledo, OH. Environ Sci Technol 51:6745–6755. https://doi.org/10.1021/acs.est.7b00856
33. Syers JK, Johnston AE, Curtin D (2008) Efficiency of soil and fertilizer phosphorus use: reconciling changing concepts of soil phosphorus behaviour with agronomic information. Food and Agriculture Organization of the United Nations, Rome
34. Team RDC (2009) A language and environment for statistical computing. Httpwww R-Proj Org
35. UNEP (2021) Making Peace with Nature: A Scientific Blueprint to Tackle the Climate, Biodiversity and Pollution Emergencies. United Nations, Erscheinungsort nicht ermittelbar
36. Yadav R, Singh S, Kumar A, Singh AN (2022) Phytoremediation: A wonderful cost-effective tool. In: Cost Effective Technologies for Solid Waste and Wastewater Treatment. Elsevier, pp 179–208
37. Zeng Z, Wu W, Ding Q, et al (2025) Overexpression of miR399d impairs arbuscular mycorrhizal symbiosis in tomato. Plant Biotechnol J 23:4381–4394. https://doi.org/10.1111/pbi.70242
38. Zhang C, Liu Y, Wang B, et al (2023) CRISPR/Cas9 targeted knockout FvPHO2 can increase phosphorus content and improve fruit quality of woodland strawberry. Sci Hortic 317:112078. https://doi.org/10.1016/j.scienta.2023.112078
39. Zulfiqar S, Gu R, Liu Y, Zhang Y (2025) From genes to traits: maximizing phosphorus utilization efficiency in crop plants. Front Plant Sci 16:1527547. https://doi.org/10.3389/fpls.2025.1527547

Figures

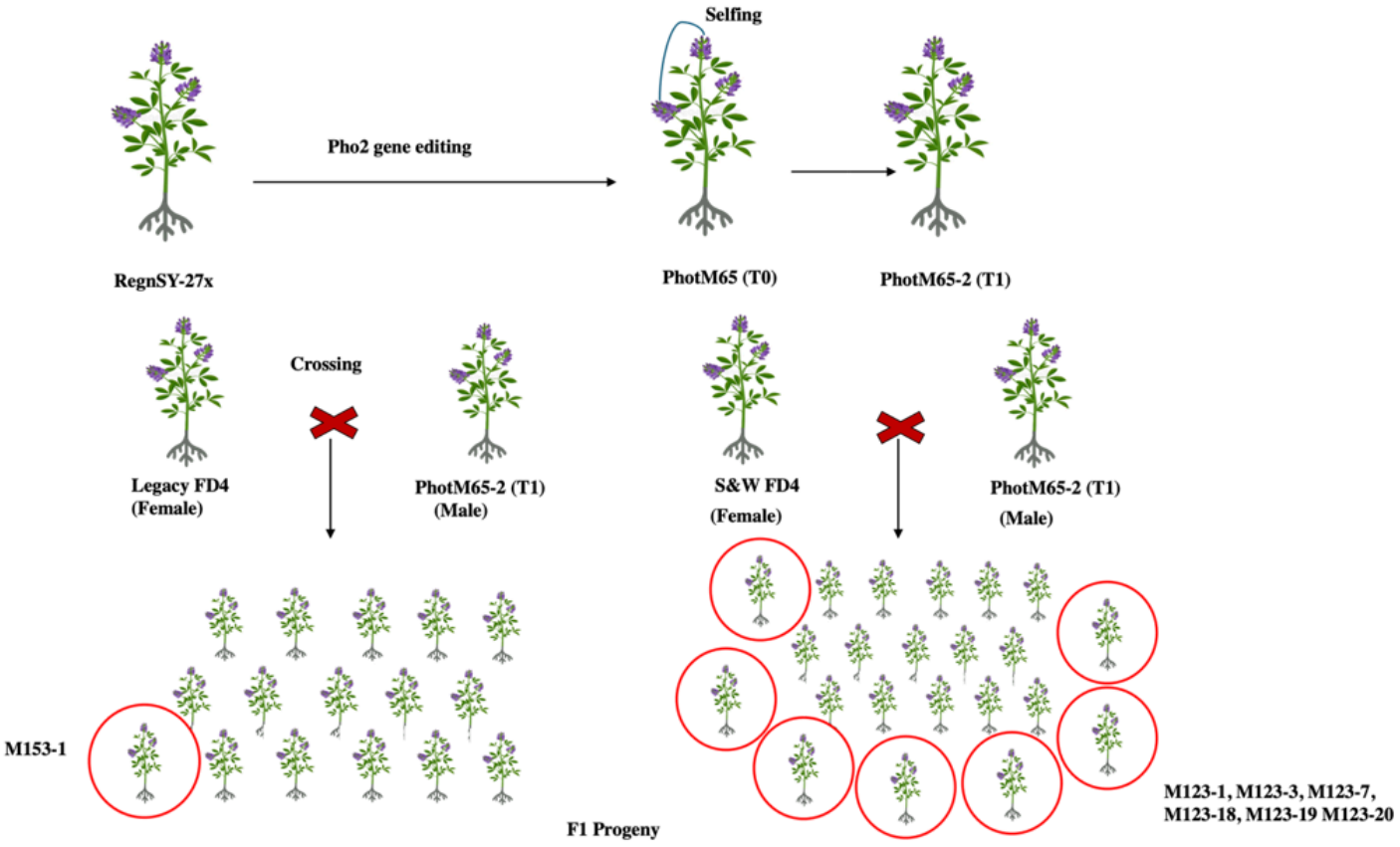

Figure 1

Schematic diagram illustrating generation of F1 progeny in alfalfa plants. RegenSY27x underwent PHO2 gene editing to produce PhotM65 (T0), which was selfed to obtain PhotM65-2 (T1). PhotM65-2 (male parent) was crossed with Legacy FD4 and S&W FD4 (female parents), resulting in F1 progeny sets: M153-1 from Legacy FD4 × PhotM65-2 (T1), and multiple lines (M123-1, M123-3, M123-7, M123-18, M123-19, M123-20) from S&W FD4 × PhotM65-2 (T1). Selected F1 alfalfa individuals are highlighted in the offspring populations as F1 progeny.

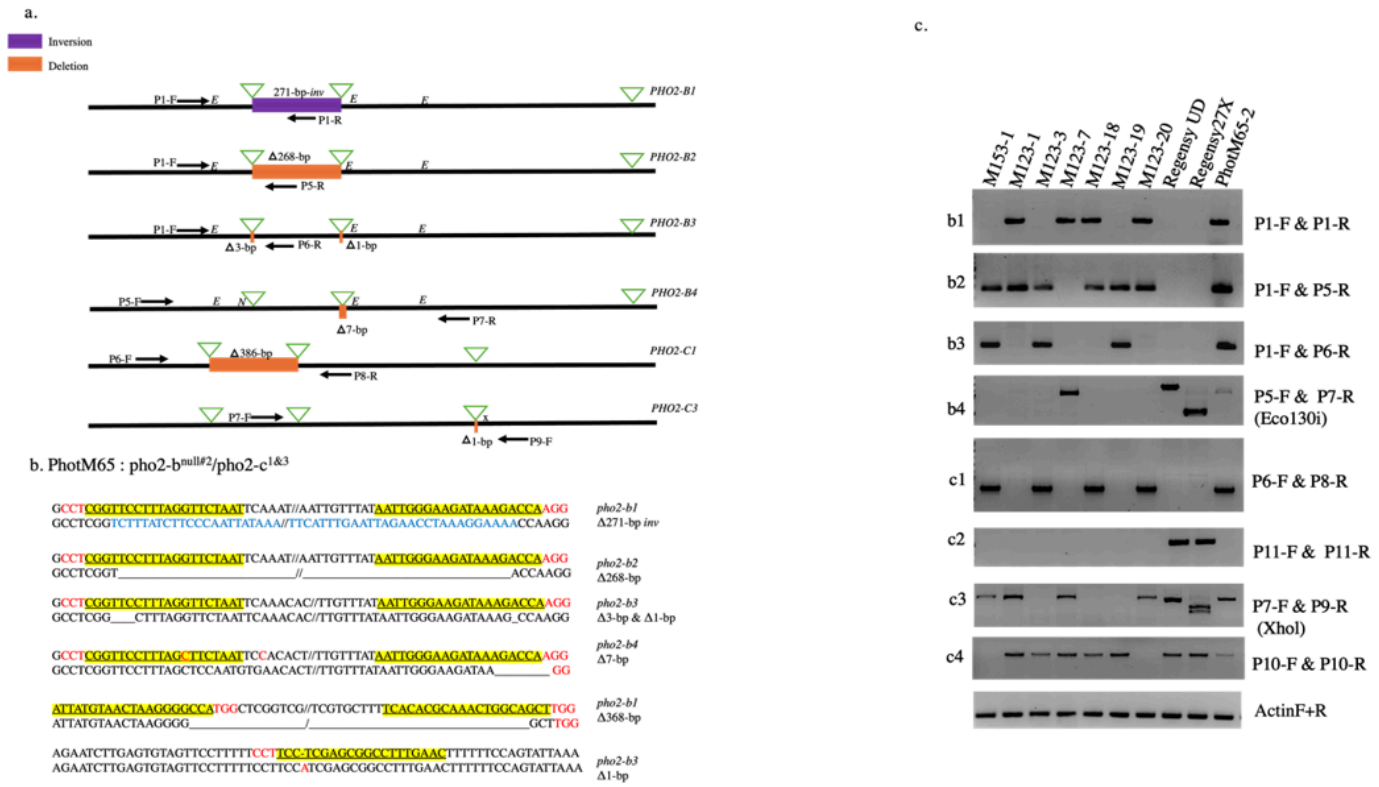

Figure 2

Identification of mutations in F1 plants. (a) Schematic representation of the PCR assays used to validate mutant haplotypes. The inverted triangles represent the reagent target sites, purple and orange boxes indicate deleted or inverted DNA sequences, respectively. The black arrows indicate the approximate primer locations used to generate amplicons. E, X, and N indicate the location of the Eco 130I, Xho I, and Nla IV restriction sites used to genotype haplotypes. (b) Sequence confirmation of the haplotypes was carried out using sequence data from the Long Amplicon Analysis (LAA) analysis as well as from cloning and sequencing assays using haplotype specific amplicons. The bold red and black text represents the PAM and target guide RNA sites for each reagent, respectively, and the blue text and black dash line indicate inverted or deleted DNA sequence. (c) Gel images of mutant and wild-type haplotype-specific amplicons from F1 mutants and donor mutant parent plant PhotM65-2 (T1) as a positive control and RegenSY27x as wildtype control. PhotM65-2 (T1) has six mutant alleles (b1, b2, b3, b4, c1 and c3) represented as the mutant specific band at the leftmost lane of gel image. The C2 wildtype allele was not detected in PhotM65-2 (T1) and similarly in F1 mutants. The absence of a haplotype specific amplicon indicates the segregation of the mutant haplotype in respective plants. The PHO2 allele is indicated on the left side of the figure. Primers and restriction enzymes used are indicated on the right side of the figure. Actin was amplified as a PCR positive control. Regensy UD, is RegenSY27x DNA without digestion. RegenSY27x is DNA with restriction enzyme digestion.

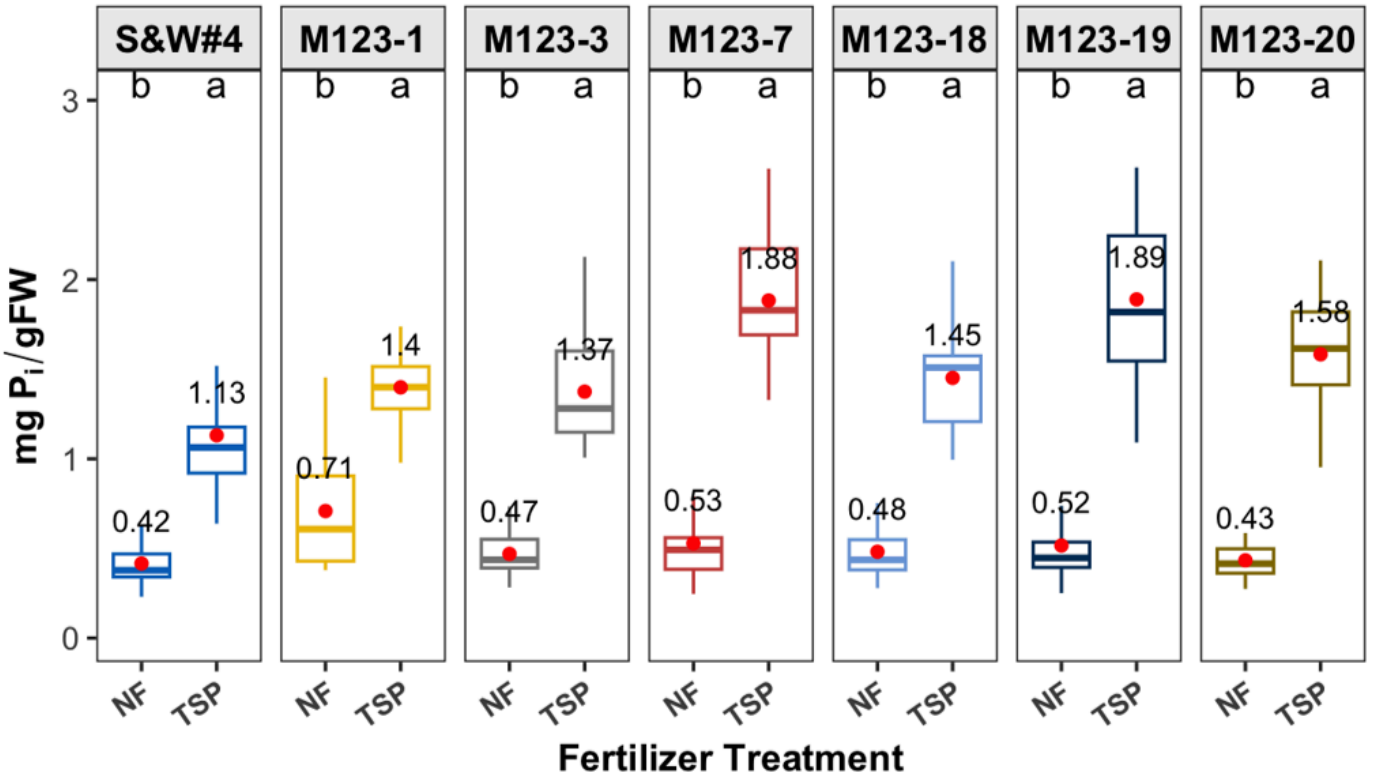

Figure 3

Foliar Pi concentration (mg g^{-1}) in the 2024 experiment under no fertilizer (NF) and triple superphosphate (TSP) treatments averaged across AMF treatments. Leaf samples were from the second node from the first harvest. Red dots indicate the mean value for each group, with numeric mean labels provided. Statistical significance within each genotype (NF vs. TSP) is indicated by LSD letter groupings (a, b).

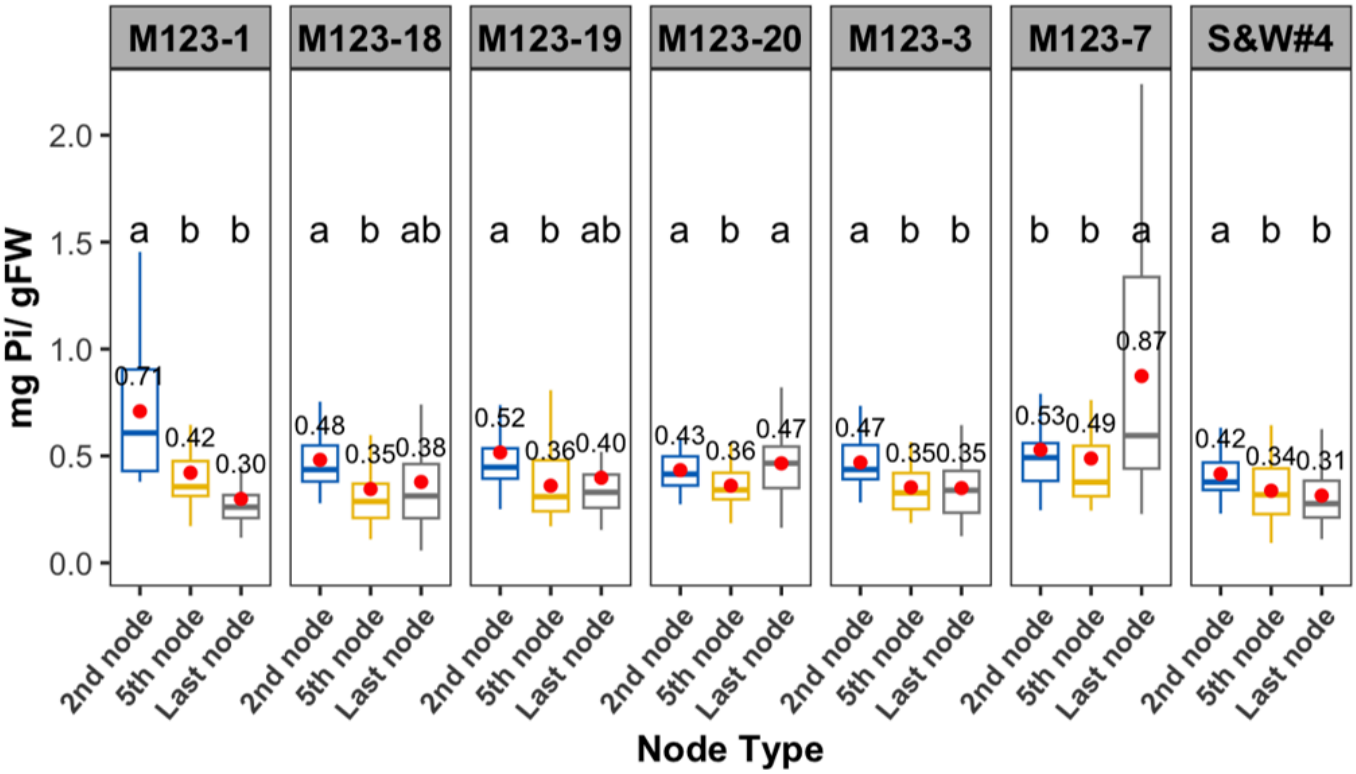

Figure 4

Spatial distribution of leaf Pi concentration across nodal positions in alfalfa genotypes at the first harvest in the NF treatment. Boxplots illustrate the Pi concentration (mg g^{-1}) at the 2nd node (youngest fully expanded), 5th node (middle), and last node (oldest/bottom). Red dots represent the mean Pi values, and numeric labels indicate mean concentrations. Statistical significance across node types within each genotype is denoted by LSD letter groupings ($P<0.05$).